Running FERMI with one-stage compressor: advantages, layout, performance.

M. Cornacchia[*], P. Craievich, S. Di Mitri*, G. Penco*,M. Venturini[**], S. Zholents***

1. Introduction

CBP-Tech Note-345 (July 2005), devoted to a study of microbunching instability in FERMI@ELETTRA linac, quotes: "… the above analysis shows that the most of the gain in microbunching instability occurs after BC2, i.e. after transformation of the energy modulation to the spatial modulation that takes place in BC2. It is possible to avoid that if we use only BC1 for all our needs for bunch compression. There are also additional advantages for a mitigation of the microbunching instability related to that. First, we would need to increase R_{56} in BC1 (for given energy chirp in the electron beam). Second, a relative energy spread is significantly larger at BC1 than at BC2. Both these factors would contribute to instability suppression due to increased Landau damping effect."

One additional argument was however missed in that report. Instability smearing due to finite emittance is stronger in BC1 simply because the geometrical emittance is larger than in BC2. In spite of the considerations in favor of a lattice with one-stage compressor, it was thought at the time that the two bunch compressors configuration was still preferable as it appeared difficult to obtain a flat-flat distribution at the end of the linac with only one bunch compressor. A flat-flat distribution has constant medium energy and a constant peak current along the electron bunch. Now, two years later and more studies behind, this problem is solvable. It has been demonstrated[1] that shaping the intensity of the electron bunch at the injector using intensity modulation of the photocathode laser allows to use the linac structural wake fields to advantage to obtain a flat-flat distribution at the end of the linac in a two-stage compressor. This report shows that, using the back-tracking technique, it is possible to obtain a flat-flat distribution also in a single-stage compressor.

Preliminary results of a study of the microbunching instability applied to the FERMI lattice with one-stage compressor are shown in this report . There is concern that the effect of jitter in accelerator parameters is more pronounced with one bunch compressor: the results of jitter studies are given and are compared with the case of a two-stage compressor.

[*] Sincrotrone Trieste S.C.p.A., Trieste, Italy.
[**] Lawrence Berkeley National Laboratory, Berkeley, California, USA.

2. Layout and Electron Beam Formation

Figure 1 shows the layout of the accelerator without the second bunch compressor (otherwise placed between Linac3 and 4).

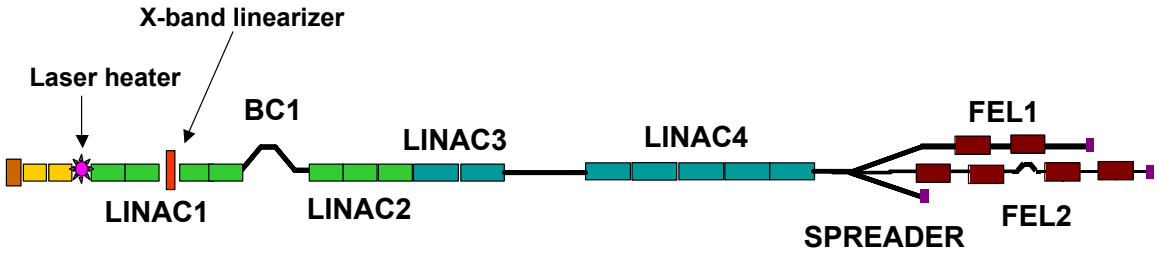

Figure 1 Layout of the accelerator with one bunch compressor.

In this configuration the energy spread and rf phases are defined by the compression factor in BC1 and the need to compensate the energy chirp with the longitudinal wakes. The parameters adopted in the "medium length bunch" configuration are shown the table.

Case	Medium Length Bunch
Elegant filename in ST server	Medium_1bc.lte
Injector filename	Medium_n8Wakes.zd
Charge (nc)	0.8
Compression ratio	14.8
Linac1: energy (MeV)	47x4
Linac1: phase (deg) from 0-crossing	42
X-band: energy	19
X-band: phase	255
Linac2: energy	47x3
Linac2: phase	72
Linac3: energy	120x2
Linac3: phase	72
Linac4: energy	120x5
Linac4: phase	60
BC1: R56 (cm)	-0.034
Laser heater (rms spread, keV)	15
Energy spread at BC1 (%,rms)	2.9
Final energy (GeV)	1.07
Final bunch length (fs, rms)	233
Final peak current (A)	~800
Final energy spread (rms, slice)	0.00019

Table 1 RF and electron beam parameters of the one-stage compressor and medium bunch configuration.

The accelerating sections Linac 2, 3 and 4 operate off crest so that the energy chirp, when added to the one needed for compression in BC1, is approximately cancelled by the longitudinal wakefield acting in the same sections. The off crest acceleration downstream of BC1 is a degree of freedom which allows one to use a smaller energy chirp in the first chicane and a correspondingly higher R56. In this way the chromatic aberrations are reduced, but the cancellation of the correlated energy spread at the end of acceleration carries a cost in final beam energy. For example, if all the chirp needed to compensate the wakefields was provided by Linac1 (with the phases of linacs 2,3 and 4 on crest) , the rms energy spread at BC1 would be 4% and the final energy 1.13 GeV. The opposite case of a large outphasing in Linac 2, 3 is discussed in the Appendix.

Figures 2-6 show the results of the Elegant simulations at the end of the spreader. The head of the bunch is on the left. It is unfortunate that the quest for a flat energy distribution leads to a current peak at the head of the bunch (as this might have unpleasant consequences due the wakefields in the undulator). In Appendix 1 a configuration is shown where the current peak occurs at the tail of the bunch at the cost of a lower final energy.

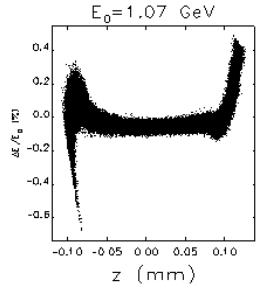

Figure 2 Longitudinal phase space

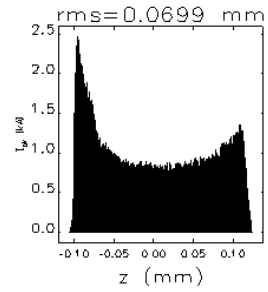

Figure 3 Current profile

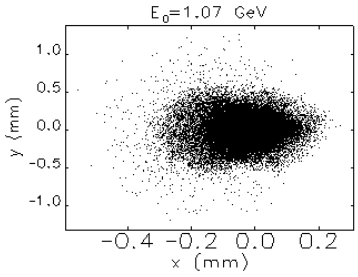

Figure 4 Transverse beam projection

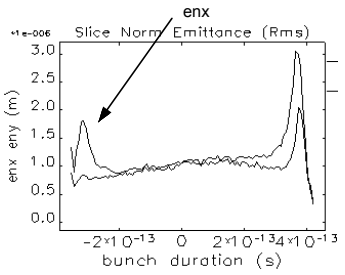

Figure 5 Horizontal (enx) and vertical normalized slice emittances

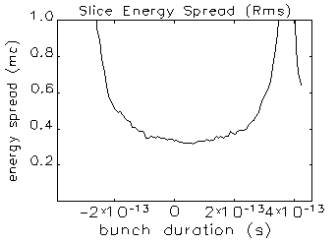

Figure 6 Slice energy spread in mc units (1 mc = 511 keV)

The simulations include longitudinal wakes and CSR effects, but no transverse electron beam displacement errors, thus no transverse wakes. The algorithm for microbunching (longitudinal space charge forces) is also not simulated. The next section is devoted to a detailed study of the microbunching instability.
The electron beam is created at the photocathode with a ramped current profile that approximates the ideal profile derived by back- current along the bunch length are shown in Figures 7 and 8.

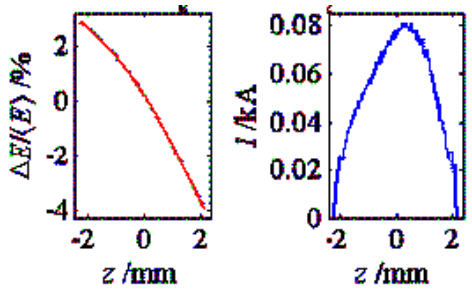

Figure 7 Desired energy and current profile at the injector end (92 MeV)

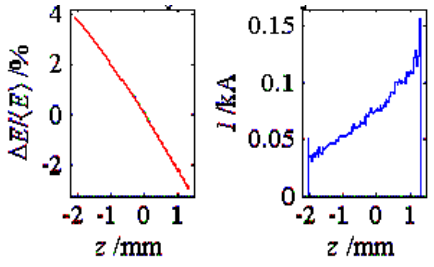

Figure 8 Actual energy and current profile

3. The Microbunching Instability with One-Stage Compressor

The computational tool used to simulate is the microbunching instability is based on the algorithm of tracking the particle distribution in 6-dimensional phase space by numerically integrating the Vlasov equation[2]. Figure 9 shows the gain of the microbunching instability with one and two bunch compressors for different values of the energy spread. The lines refer to the linear theory[3] and the points are the results of the Vlasov Solver. Both CSR and longitudinal space charge were simulated in the Vlasov Solver, with the latter being the dominant effect. The gain of the instability is dramatically reduced with one bunch compressor, and why it should be so deserves a discussion.

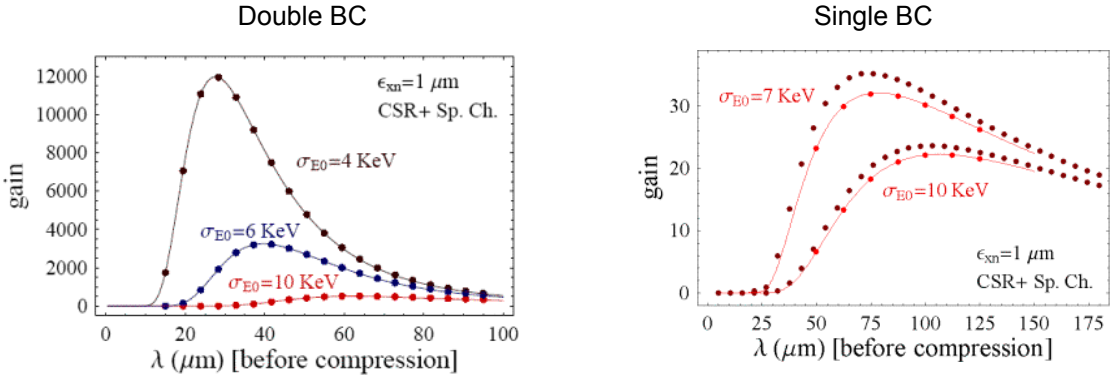

Figure 9 Gain of the microbunching instability with and one and two bunch compressors

Compared to the Two-BC-lattice the beam of One_BC-lattice experiences longer sections of linac at higher peak current (detrimental) but with a larger uncorrelated energy spread (beneficial). The energy spread increases by the bunching factor of the compressor, ie about a factor 10. The energy spread wins, as the gain becomes exponentially small at larger energy spreads according to the formula[4]

$$b \sim C^2(s)\exp\left(-k_0{}^2 R_{56}(s) C^2(s)\sigma_\delta{}^2\right) \qquad \textbf{(1)}$$

Figure 10 depicts the rms energy spread at the end of the linac with one bunch compressor as a function of the energy spread induced by the laser heater. The simulations give <120 KeV final energy spread for a 9.5 KeV rms energy spread produced by the spreader at 100 MeV. This is a very satisfactory result, as 120 keV is well within the FEL tolerance for this parameter[5].

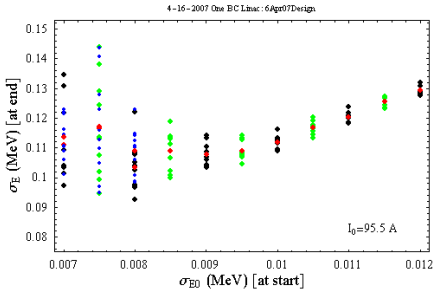

Figure 10 Energy spread at the end of acceleration as a function of the laser heater induced spread.

4. Jitter Studies

It is to be expected that the sensitivity of the electron beam characteristics to changes in accelerator parameters is more pronounced with one stage compressor compared to two. A statistical study of the effect of changes in accelerator parameters was carried out and compared to the results of a two stage compressor.
The technique applied to the study is described in reference[6]. Table 1 lists the tolerances of relevant rf parameters that need to be met together in order to limit the total electron beam jitters to less than (rms values):

- 10% in peak current
- 0.1% in energy deviation
- 150 fs time jitter

The table indicates that a single stage compressor tightens the tolerances, but, overall, less than a factor 2.

Parameter	Sy.	Unit	2BC	1BC
C1-C4 RF phase (L1)	$\varphi 1$	deg	**0.10**	**0.05**
X band phase (LX)	φx	deg	**0.30**	**0.35**
C5-C7 RF phase (L2)	$\varphi 2$	deg	**0.10**	**0.20**
S1-S2 RF phase (L3)	$\varphi 3$	deg	**0.10**	**0.15**
S3-S7 RF phase (L4)	$\varphi 4$	deg	**0.10**	**0.10**
C1-C4 RF voltage (L1)	$\Delta V_1/V_1$	%	**0.10**	**0.10**
X band voltage (LX)	$\Delta Vx/Vx$	%	**0.50**	**0.30**
C5-C7 RF voltage (L2)	$\Delta V_2/V_2$	%	**0.10**	**0.15**
S1-S2 RF voltage (L3)	$\Delta V_3/V_3$	%	**0.10**	**0.08**
S3-S7 RF voltage (L4)	$\Delta V_4/V_4$	%	**0.05**	**0.05**
Gun timing jitter	Δt_0	psec	**0.25**	**0.35**
Initial bunch charge	$\Delta Q/Q$	%	**3.00**	**5.00**
BC1 chicane	$\Delta B_1/B_1$	%	**0.02**	**0.01**
BC2 chicane	$\Delta B_2/B_2$	%	**0.02**	**-**

Table 1 Tolerance budget of rf parameters with one and two bunch compressors.

Looking at this issue from a different angle, figure 11 depicts the results of a statistical study that uses the technique of Latin Hypercube Sampling where the parameters of Table 2 were randomly varied with rms values of Gaussian distribution shown in the tolerance column. This study was made in order to obtain a more direct comparison between the two configurations. Taking the results from Figure 11, we have, for the rms values of the resulting variations:

- Peak current
  - Single compressor: 11.4 %
  - Double compressor: 7.9 %
- Energy deviation
  - Single: 0.11 %
  - Double: 0.12 %
- Time jitter
  - Single: 175 fs
  - Double: 129 fs

Single-stage compressors Double-stage compressor

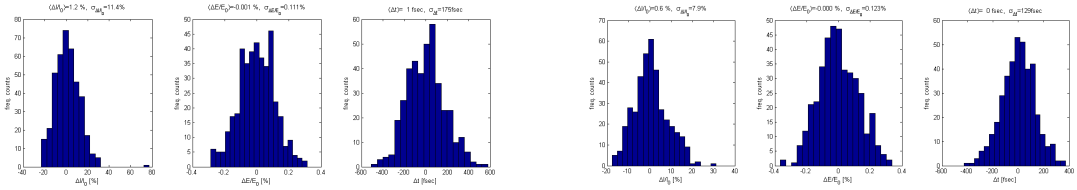

Figure 11 Distributions of peak current, relative energy and time jitters consequent to random rms changes of rf parameters listed in Table 2.

Parameter	Sy.	Unit	tol
C1-C4 RF phase (L1)	$\varphi 1$	deg	**0.10**
X band phase (LX)	φx	deg	**0.30**
C5-C7 RF phase (L2)	$\varphi 2$	deg	**0.10**
S1-S2 RF phase (L3)	$\varphi 3$	deg	**0.10**
S3-S7 RF phase (L4)	$\varphi 4$	deg	**0.10**
C1-C4 RF voltage (L1)	$\Delta V_1/V_1$	%	**0.10**
X band voltage (LX)	$\Delta Vx/Vx$	%	**0.40**
C5-C7 RF voltage (L2)	$\Delta V_2/V_2$	%	**0.10**
S1-S2 RF voltage (L3)	$\Delta V_3/V_3$	%	**0.10**
S3-S7 RF voltage (L4)	$\Delta V_4/V_4$	%	**0.10**
Gun timing jitter	Δt_0	psec	**0.25**
Initial bunch charge	$\Delta Q/Q$	%	**5.00**
BC1 chicane	$\Delta B_1/B_1$	%	**0.01**
BC2 chicane	$\Delta B_2/B_2$	%	**0.01**

Table 2 Table of parameters and tolerances used for the comparison of Figure 11.

5. Conclusions

This report re-examines the option of running the FERMI FEL driver with a single-stage compressor. This configuration offers the unique advantage of essentially degrading the microbunching instability to the point where it is not longer a threat to the performance of the FEL. There is a small price to pay in terms of enhanced sensitivity to changes of some rf parameters.

6. Appendix

The system acceleration-energy chirp cancellation offers one degree of freedom for a given compression ratio. For instance, once R56 is set, the energy spread at BC1 is determined and so are the rf phases in linacs 2,3 and 4. The configuration of Table 1 chooses a moderate R56 in order to keep the final energy above 1 GeV. If a lower energy was acceptable by the FEL process and its applications, a configuration is possible whereby the energy spread at the compressor is reduced, no outphasing of the x-band structure is necessary and the current peak takes harmlessly place at the head of the bunch.

Case	Medium Length Bunch
Elegant filename in ST server	
Injector filename	Medium_n8Wakes.zd
Charge (nc)	0.8
Compression ratio	14.5
Linac1: energy (MeV)	47x4
Linac1: phase (deg) from 0-crossing	52
X-band: energy	19
X-band: phase	270

Linac3: energy	120x2
Linac3: phase	50
Linac4: energy	120x5
Linac2: energy	47x3
Linac2: phase	50
Laser heater (rms spread, keV)	15
Energy spread at BC1 (%,rms)	2.5
Final energy (GeV)	0.958
Final bunch length (fs, rms)	190
Final peak current (A)	~900
Final energy spread (rms, slice)	~0.00033

Figures 12-16 show the results of the Elegant simulations at the end of the spreader. The current peak now is at the tail of the bunch.

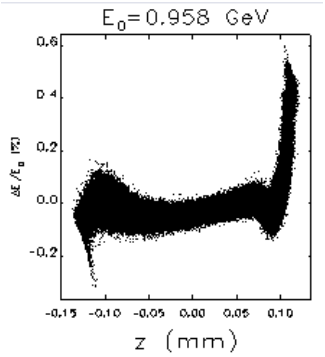

Figure 12 Longitudinal phase space

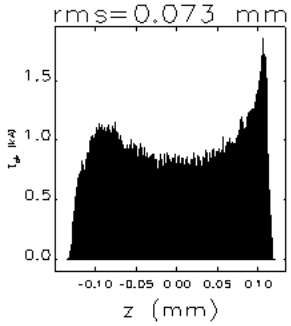

Figure 13 Current profile

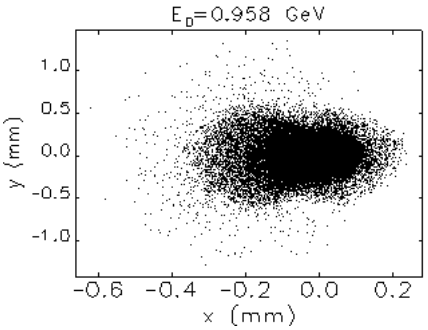

Figure 14 Transverse beam projection

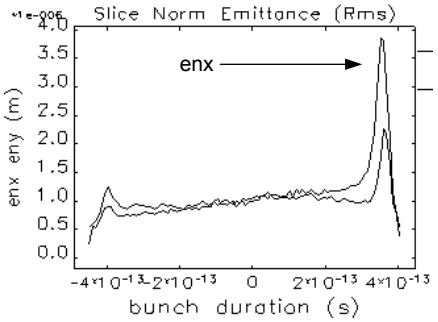

Figure 15 Horizontal (enx) and vertical normalized slice emittances

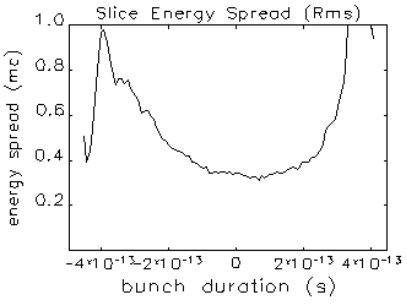

Figure 16 Slice energy spread in mc units (1 mc = 511 keV)

[1] M Cornacchia et.al., Phys. Rev. Special Topics – Acc. And Beams, 9, 120701 (2006).
[2] M. Venturini, R. Warnock, A. Zholents, to be published in PRST-AB, (2007)
[3] Y. Derbenev, V. Shiltsev, SLAC-PUB-7181 (1996)
[4] Z. Huang and K.-J. Kim, PRST-AB, 5, 074401 (2002).
[5] FERMI@Elettra CDR, Chapter 4, Table 4.4.1, to be published
[6] P. Craievich et al., "Jitter Studies for the FERMI Linac", Proc. EPAC Conf. 2006.